

A broad spectrum analysis of the dielectric properties of poly(2-hydroxyethyl methacrylate)

K. Mohamed^a, T.G. Gerasimov^a, F. Moussy^b, J.P. Harmon^{a,*}

^aDepartment of Chemistry, University of South Florida, 4202 East Fowler Avenue, Tampa, FL 33620-5250, USA

^bDepartment of Chemical Engineering, University of South Florida, 4202 East Fowler Avenue, Tampa, FL 33620-5250, USA

Received 9 December 2004; accepted 22 February 2005

Available online 7 April 2005

Abstract

The dielectric permittivity, ϵ' , and the loss factor, ϵ'' , of dry poly(2-hydroxyethyl methacrylate) were measured using a dielectric analyzer in the frequency range of 0.1 Hz to 100 kHz and between the temperature range of -150 to 275 °C. The dielectric response of the sub- T_g γ transition of PHEMA has been widely studied before but little to no DEA data above 50 °C is present in the literature. In this study the dielectric spectrum is presented up to and above the T_g . The electric modulus formalism is used to reveal the γ , β , α and conductivity relaxations. The apparent activation energies for the relaxations are presented.

© 2005 Elsevier Ltd. All rights reserved.

Keywords: PHEMA; Conductivity relaxation; Electric modulus

1. Introduction

1.1. Poly(2-hydroxyethyl methacrylate)

Poly(2-hydroxyethyl methacrylate) (PHEMA) belongs to the class of polymers known as hydrogels. When such polymers are crosslinked they swell in water and retain a significant fraction of water without dissolving [1,2]. PHEMA is a widely studied polymer that has found its niche in the bioapplications field; it is included as materials for contact lenses, bioadhesive gels for drug delivery applications, and thrombo- and fibro-resistant coatings [3–6]. PHEMA also has a great potential as a protective/interactive coating on the surface of implantable biosensors. However, new applications in semi-conducting nanocomposite host–guest systems in our laboratory obviated the need to further characterize the dielectric behavior of neat PHEMA.

In this study the dielectric response of dry PHEMA from -150 to 275 °C is presented. The dielectric response of dry and hydrated PHEMA have been studied before but data

obtained above 50 °C have not been previously reported [3, 7–12]. In mechanical studies dry PHEMA exhibits two sub- T_g secondary relaxations and a primary glass transition. The transitions are termed α , β , and γ proceeding from the high temperature transition to the low temperature transition. The primary α transition marks the onset of large scale segmental motion of the main chain, or polymer backbone, and in the case of hydrogels it is affected by factors such as the degree of crosslinking and water content. The β relaxation corresponds to the rotation of the ester side group and the γ relaxation is associated with the rotation of the hydroxyethyl group [3,12,13]. An additional relaxation, β_{sw} , is observed in hydrated PHEMA at a temperature slightly greater than the γ transition; β_{sw} corresponds to the motion associated with the interaction of the water molecules with the side groups in the polymer [3,12–15]. Mechanical studies have shown that the γ relaxation is very pronounced whereas the β relaxation is relatively weak. The β relaxation often appears as a shoulder to the α peak and may even be unresolvable [3,9,12,13].

In 1979, Diaz Calleja extensively studied the lower region of the dielectric spectra of PHEMA in which the γ relaxation was characterized [7]. Due to instrument constraints, high temperature data points were unattainable but the presence of a second loss peak was detected and it was suggested that the higher temperature peak observed

* Corresponding author. Tel.: +1 813 974 3397; fax: +1 813 974 1733.
E-mail address: harmon@cas.usf.edu (J.P. Harmon).

may be attributed to the β relaxation [7]. Then in 1984, Gomez Ribelles and Diaz Calleja became the first to present dielectric data on the β relaxation of PHEMA in which they observed a dielectric loss peak at ca. 50 °C (0.02 Hz) with an activation energy of 29 kcal/mol [8]. The intramolecular hydrogen bonding between the polar –OH groups attached to the polymer chains hinders motion of the ester moiety and requires a higher energy input to onset the relaxation which is evidenced by a high temperature loss peak and high activation energy [8,9].

Three different processes were observed in this study taking place at ca. 50 °C and above and, due to the paucity of DEA data in literature covering this temperature range an attempt was made to decipher the meaning of the dielectric spectrum of dry PHEMA. This study is important because dielectric behavior gives insight into not only the structural property and relaxations present in the polymer but can also be used to investigate the conductivity and interaction of the polymer with nanofillers which is of current interest.

1.2. Dielectric theory and analysis

DEA is an informative technique used to determine the molecular motions and structural relaxations present in polymeric materials possessing permanent dipole moments [16,17]. In dielectric measurements the material is exposed to an alternating electric field, that is generated by applying a sinusoidal voltage; this process causes alignment of dipoles in the material, which results in polarization. The polarization will cause the output current to lag behind the applied electric field by a phase shift angle, θ . The magnitude of the phase shift angle is determined via measuring the resulting current. The capacitance and conductance are then calculated from the relationship between the applied voltage, measured current and phase shift angle [16–18]. The capacitance and conductance of the material are measured over a range of temperature and frequency, and are related to the dielectric permittivity, ϵ' , and the dielectric loss factor, ϵ'' , respectively. The dielectric permittivity, ϵ' , represents the amount of dipole alignment (both induced and permanent) and the loss factor, ϵ'' , measures the energy required to align dipoles or move ions. The dielectric permittivity and the loss factor are the real and imaginary components of the complex permittivity, ϵ^* , given by

$$\epsilon^* = \epsilon' - i\epsilon'' \quad (1)$$

In polymeric materials it has been observed that the loss factor term is a combination of two processes which are dependent on temperature, pressure and density:

1. The rotational reorientation of the permanent dipoles present on the side chains off the polymer backbone, known as a dipolar relaxation. This process is viscoelastic and usually exhibits a loss peak that is close to symmetric in shape and obeys Arrhenius behavior for

secondary relaxations [19–21]. The glass transition also contributes to the loss function as a result of the induced dipoles created by the redistribution of electrons shared between the bonded atoms on the main chain [16,17].

2. The translational diffusion of ions which causes conduction is seen as a conductivity relaxation. In glass forming polymers this process takes place with increasing viscous flow and usually overpowers the viscoelastic α process in the dielectric loss factor spectrum [20–23]. As temperature increases it has been shown that the loss factor becomes inversely proportional to frequency. The AC conductivity, σ , is given by Eq. (2), where ω is the angular frequency and ϵ_0 is the absolute permittivity of free space (8.854×10^{-12} F/m).

$$\sigma_{Ac} = \epsilon'' \omega \epsilon_0 \quad (2)$$

McCrum et al. have formulated a mathematical treatment of the complex permittivity, ϵ^* , which is used to resolve the viscoelastic α process from the conductivity effects [16]. By taking the inverse of the complex permittivity, ϵ^* , one can obtain the complex electric modulus given by Eq. (3).

$$M^* = \frac{1}{\epsilon^*} = M' + iM'' = \frac{\epsilon'}{\epsilon'^2 + \epsilon''^2} + i \frac{\epsilon''}{\epsilon'^2 + \epsilon''^2} \quad (3)$$

Plots of the electric loss modulus, M'' , versus temperature show a significant difference from those of ϵ'' versus temperature plots with respect to the separation of the viscoelastic and conductivity relaxations, but technically contain the same information [23]. Due to the placement of the dielectric constant, ϵ' , in the denominator of the equation, its effect in dominating M' and M'' is reduced [19,23]. This allows a more comprehensive analysis of the dielectric data.

The conductivity relaxation possesses properties very different from the viscoelastic relaxations present in polymers. The conductivity relaxation corresponds to the model of a Debye process having a single relaxation time, whereas viscoelastic relaxations are known to exhibit a distribution of relaxation times [16,17]. In this paper various mathematical treatments will be applied to reveal both the viscoelastic and conductivity relaxations present in the dielectric spectrum of PHEMA.

2. Experimental

2.1. Materials

2-Hydroxyethyl methacrylate monomer was generously donated by Benz R&D (Sarasota, FL). It was used as received without further purification. The free radical initiator employed for the polymerization was Vazo 52[®] [2,2',-azobis(2,4-dimethylpentane nitrile)]. Vazo 52[®], obtained from Dupont (Wilmington, DE), is a low

temperature polymerization initiator that decomposes to form a cyanoalkyl radical.

2.2. Synthesis of PHEMA

0.2 wt% of the [2,2',-azobis(2,4-dimethylpentane nitrile)] Vazo 52[®] initiator was added to the monomer which was then degassed with dry nitrogen gas. The monomer was polymerized for 8 h at 60 °C and then post cured at 110 °C for 4 h. Before thermal, mechanical and dielectric analysis, the PHEMA sample was oven dried at 110 °C to constant weight under vacuum and stored under vacuum in the presence of phosphorous pentoxide. It should be noted that the monomer contained a small amount of dimethacrylate impurity, which resulted in the crosslinking of the polymer. The polymer had the ability to be molded but not dissolved.

2.3. Differential scanning calorimetry

Experiments were performed on a TA Instruments DSC 2920 to determine the glass transition temperature, T_g , of PHEMA. The previously dried sample (4–10 mg) was hermetically sealed in an aluminium pan and a heat-cool-heat cycle was performed. The DSC cell, which was calibrated with indium and kept under an inert nitrogen atmosphere, was heated using a ramp rate of 5 °C/min to 140 °C, quench cooled with liquid nitrogen and then reheated at the same rate. The T_g was taken from the second heating cycle.

2.4. Thermogravimetric analysis

A TA Instruments HiRes TGA 2950 was used to determine both the decomposition temperature of PHEMA as well as to determine if the drying technique used resulted in complete removal of absorbed water from the polymer. The data was obtained under a dry nitrogen purge at a ramp rate of 20 °C/min from 30 to 400 °C.

2.5. Sample molding

Samples were compression molded using a Carver Press equipped with a heating element at a temperature of 135 °C for 5 min; it was then air cooled under pressure to room temperature. DEA samples were molded into rectangular disks with dimensions of 25 × 20 × 1 mm³. The DMA samples were molded into rectangular pieces of 30 × 6 × 1 mm³. Molded samples were then vacuum oven dried at 60 °C until constant mass and then stored under vacuum in the presence of phosphorous pentoxide until ready to use.

2.6. Dynamic mechanical analysis

Dynamic mechanical analysis was conducted on a TA Instruments DMA 2980. The instrument and clamps were

calibrated and the experiments were run under tension mode. Measurements with an oscillating amplitude of 5 μm were taken from –150 to 200 °C in 5° increments through a frequency range of 1–100 Hz. A preload force of 0.010 N was used to maintain sample tension and the force tracking option of 125% was used to automatically adjust the force as the sample changed modulus in order to minimize sample deformation. The storage modulus (E'), loss modulus (E'') and mechanical loss tangent ($\tan \delta$) were obtained.

2.7. Dielectric analysis

Single surface dielectric analysis was performed using a TA Instruments DEA 2970. The sample was heated to 135 °C to embed the sample into the channels of the single surface sensor and then taken down to cryogenic temperatures with liquid nitrogen. A maximum force of 250 N was applied to the sample to achieve a minimum spacing of 0.25 mm. Measurements were taken in 5° increments from –150 to 275 °C through a frequency range of 0.1 Hz to 100 kHz under a dry helium atmospheric purge of 500 ml/min. Capacitance and conductance were measured as a function of time, temperature and frequency to obtain the dielectric constant, or permittivity (ϵ'), the dielectric loss (ϵ'') and the loss tangent ($\tan \delta = \epsilon''/\epsilon'$).

3. Results and discussion

3.1. DSC and TGA

DSC was used to monitor the drying process since the presence of water in the hydrophilic polymer is known to act as a plasticizer which will decrease the glass transition temperature. The drying process was complete when the T_g remained constant even after additional heating under vacuum. DSC was used to determine the glass transition temperature of PHEMA, it was found to have a T_g of 99.2 °C. A decomposition temperature of 330 °C was determined by thermogravimetric analysis. Minimal water content was observed as there was only a 0.5% weight loss up to 120 °C. The dielectric analysis was taken up to 275 °C, a temperature at which there was a 6% weight loss.

3.2. DMA

The mechanical viscoelastic relaxations in PHEMA have been previously reported [3,10–13,24]. Dry PHEMA exhibits two sub- T_g relaxations, the γ relaxation which is associated with the rotation of the hydroxyethyl group and β relaxation corresponding to the rotation of the ester side group.

3.2.1. γ relaxation

Our DMA experiment confirms a γ transition occurring between a temperature range of –135 to –116 °C for the

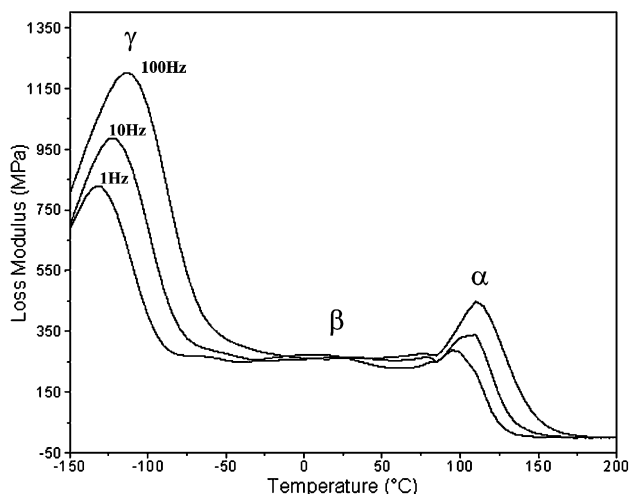


Fig. 1. DMA data: loss modulus (E'') vs. temperature for PHEMA.

frequency range of 1–100 Hz. It follows Arrhenius behavior and has an activation energy of 10.6 kcal/mol (44.4 kJ/mol). This is compared to previously reported values of a γ transition occurring at -133 °C (1 Hz) with an activation energy of 10.7 kcal/mole (44.8 kJ/mol) and -132 °C (1 Hz) with an activation energy of 7.5 kcal/mole (31.4 kJ/mol) [3,13].

3.2.2. β relaxation

The β relaxation is only observed at 1 Hz as it is overlapped by the α relaxation as shown in Fig. 1. Kolarik observed the β transition in dry PHEMA at 26.9 °C (1 Hz) and Gates observed the β transition at 28 °C (1 Hz).

DMA in correlation with DEA has been used to best describe the relaxations exhibited in PHEMA. The mechanical and dielectric relaxations in PHEMA are not as closely related as one would think. The β relaxation has been observed to be more pronounced in DEA than in

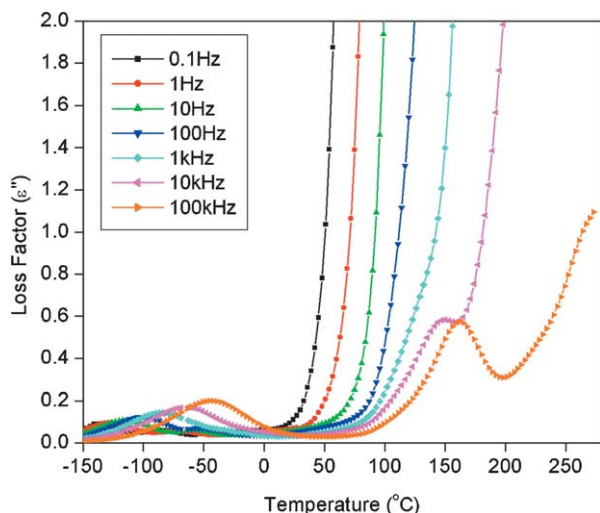


Fig. 2. DEA data: loss factor (ϵ'') vs. temperature for PHEMA.

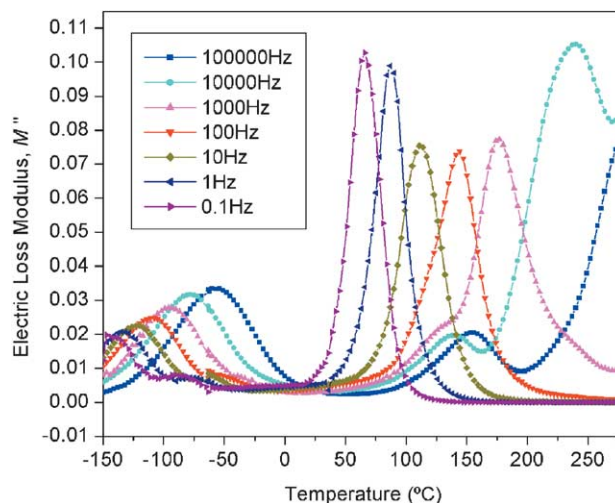


Fig. 3. DEA data: electric Loss Modulus (M'') vs. temperature for PHEMA.

DMA; this point is discussed in greater detail in a later section.

3.3. DEA

DEA analysis of PHEMA revealed anomalous behavior which has not been reported by researchers who studied the dielectric properties of this polymer. Most of the work published present data up to 50 °C in which detailed analyses of the γ transition are presented. The γ , β , possible α (or $\alpha\beta$ merge) and the conductivity relaxations present in PHEMA have been identified with DEA. Fig. 2 shows the loss factor plot of PHEMA and Fig. 3 shows the electric loss modulus plot. The γ transition is clearly observed; however, the occurrence of ionic conduction in the sample has hidden the β and α transitions in the ϵ'' plot. By applying the electric modulus formalism the β and α relaxations are revealed.

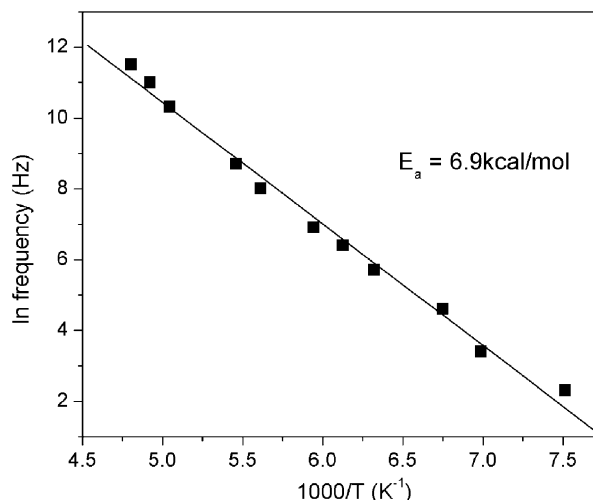


Fig. 4. Arrhenius plot of γ relaxation in PHEMA.

3.3.1. γ relaxation

The γ relaxation appears as a strong peak in both the loss factor and electric loss modulus plots. It obeys Arrhenius behavior where the peak temperature maxima increased linearly with frequency as shown in the Arrhenius plot of $\ln f$ vs. the reciprocal of temperature (Fig. 4); the slope of which was used to determine the activation energy from the relationship [16,25,26] of

$$\ln f = \ln f_0 - \frac{\Delta E_a}{RT} \quad (4)$$

The γ relaxation occurs within a temperature range of -147 to -60 °C (0.1 Hz–100 kHz) and has an activation energy of 6.9 kcal/mol (28.9 kJ/mol) as determined from the electric loss modulus temperature maxima Arrhenius dependence. Both the activation energy, as well as the temperature, of the dielectric γ relaxation is lower than the measured mechanical γ relaxation as shown in Table 1. This occurrence has been reported previously by Gates et al. and Janacek. It can be explained by the concept of mechanical activation versus dielectric activation. Rotation of the $-OH$ side group in PHEMA is observed as a result of (1) slow viscoelastic deformation on the application of a mechanical load and (2) slow orientation polarization on the application of an electric field. The viscoelastic deformation is weakly dependent on the dipole moment of the $-OH$ side group whereas the orientation polarization is strongly dependent on the dipole moment [27,28]. The dipole moment of the $-OH$ group is large and appears to be more easily aligned in the electric field, whereas in DMA the energy needed to overcome the dispersive Van der Waals forces to allow rotation of the $-OH$ group is greater.

Previously reported activation energy values for the γ relaxation range from 6.9 to 16 kcal/mol. As mentioned by Pathmanathan and Johari this may be caused by the different crosslinking density of the polymer; the higher the crosslinking density the higher the activation energy needed to overcome hindered rotation of the $-OH$ side group [10,11].

3.3.2. α and β relaxations

Until now the dielectric β relaxation in PHEMA has only been reported by Gomez Ribelles and Diaz Calleja in which they reported a loss peak at 50 °C (0.02 Hz) with an activation energy of 29 kcal/mol (121 kJ/mol) [8]. Further data at higher temperatures and frequencies were not presented. As observed in the loss factor plot (Fig. 2) the β and α relaxations were obscured by conductivity effects so the electric modulus formalism was used; in the ϵ'' plot the

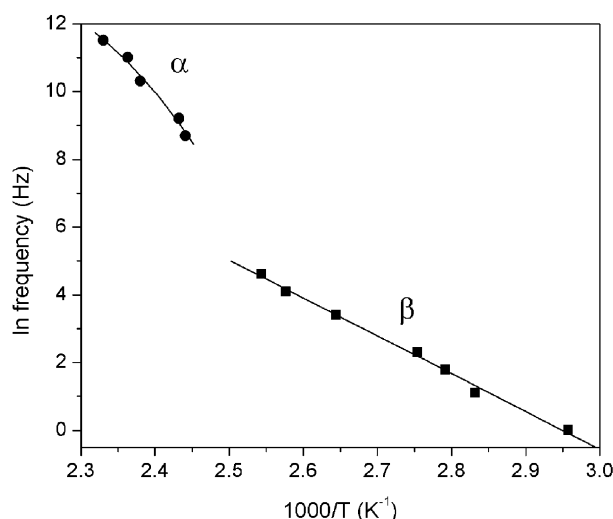


Fig. 5. Arrhenius plots of the α and β relaxations.

α , or possible $\alpha\beta$ merge, peak was only observed at high frequencies (6–100 kHz) at ca. 145–160 °C.

It was interesting to observe the anomalous behavior exhibited in the electric loss modulus vs. temperature plot as shown in Fig. 3. Frequency scans from 0.1 to 10 Hz show a symmetric, single electric modulus loss peak between the temperature range of 66–113 °C. This peak follows Arrhenius behavior in which the peak temperature maxima increased linearly with frequency to give an activation energy of 20.7 kcal/mol (86.7 kJ/mol). One may argue that this is the α peak corresponding to the glass transition temperature but experimental data prove otherwise. The symmetry and Arrhenius relationship are characteristic of secondary relaxations [16]. The frequency–temperature dependence of the β and α peaks is shown in Fig. 5.

As the frequency is increased two M'' peaks are apparent. The first peak appears first as a shoulder to the second peak for frequencies 300 Hz to 1 kHz and then as a separate peak from 3 to 100 kHz. The first M'' peak occurs at a peak height significantly lower than the one M'' peak observed in the lower frequencies and is attributed to the α , or possible $\alpha\beta$ merge. It is not symmetric and does not follow Arrhenius behavior. One can reason that the β relaxation requires a higher temperature to initiate the rotation of the lateral side group due to the presence of intramolecular bonding. In poly(methylmethacrylate) the β relaxation is faster moving than the α relaxation and tends to merge with the α relaxation at a temperature above T_g [16,21]. In PHEMA, the β relaxation may have overlapped with the α relaxation to form the $\alpha\beta$ merge which is seen as the first M'' peak in

Table 1
DEA vs. DMA for the γ transition

Properties	DEA	DMA
γ peak at 1 Hz (obtained from $\tan \delta$ plot)	-130.14 °C	-124.56 °C
E_a (obtained from ϵ'' , E' plots)	6.9 kcal/mol	10.6 kcal/mol

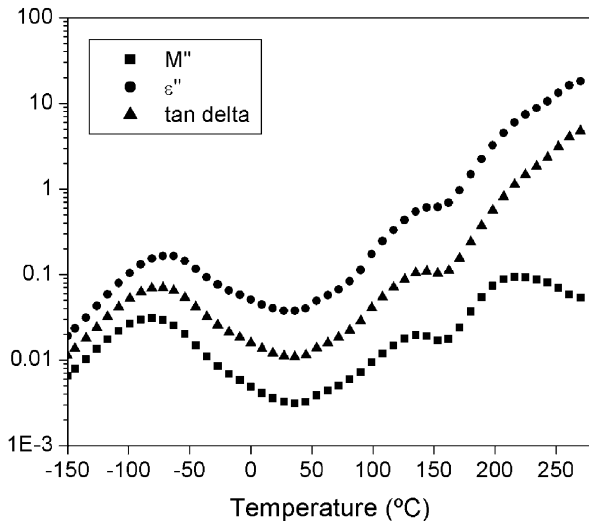


Fig. 6. Dielectric loss functions of PHEMA at 6 kHz.

the higher frequency scans. Fig. 6 shows the electrical loss functions for comparison of dry PHEMA at 6 kHz.

3.3.3. Conductivity relaxation

Upon mathematically treating the ϵ'' data to obtain the electric loss modulus (M'') several changes occur. The dielectric permittivity, ϵ' , increases dramatically with increasing temperature and frequency; in electric modulus the placement of the dielectric constant, ϵ' , in the denominator of the equation prevented it from dominating M' and M'' . It is also observed that the M'' peaks, especially for the γ transition, occurred at temperatures lower than the ϵ'' peaks. By taking the electric modulus the space charge effects are suppressed and an ionic conductivity peak is revealed [23,29,30]. This is seen as the second M'' peak in the spectra for the higher frequency scans. The fact that this is a conductivity relaxation and not a viscoelastic relaxation can be proven in several ways.

Proof 1. The dielectric permittivity and loss factor for a relaxation with a single relaxation time can be described by Eqs. (5) and (6),

$$\epsilon' = \epsilon_U + \frac{(\epsilon_R - \epsilon_U)}{1 + \omega^2 \tau_E^2} \quad (5)$$

$$\epsilon'' = (\epsilon_R - \epsilon_U) \frac{\omega \tau_E}{1 + \omega^2 \tau_E^2} \quad (6)$$

where τ_E is the dielectric relaxation time, ω is the angular frequency, and ϵ_U and ϵ_R represents the high frequency, unrelaxed state and the low frequency, relaxed state, respectively. By manipulating Eqs. (5) and (6), Eq. (7) is derived.

$$\left\{ \epsilon' - \frac{(\epsilon_R + \epsilon_U)}{2} \right\}^2 + (\epsilon'')^2 = \left(\frac{\epsilon_R - \epsilon_U}{2} \right)^2 \quad (7)$$

Cole and Cole proposed that by plotting ϵ'' against ϵ' at a

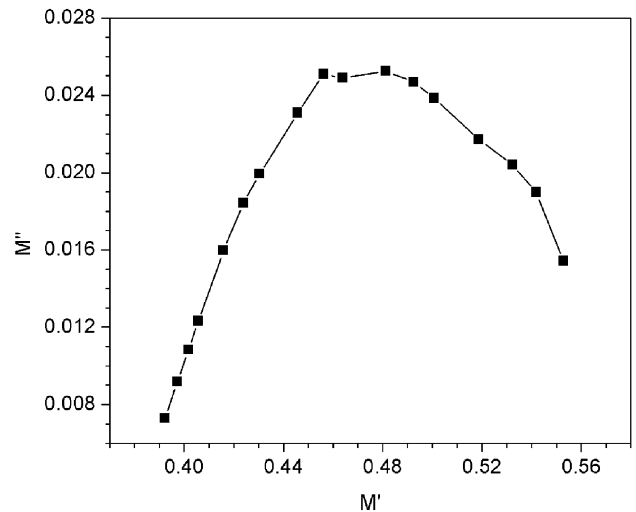


Fig. 7. Argand plot derived from γ relaxation region (-110°C).

particular temperature, a semicircle of radius $(\epsilon_R - \epsilon_U)/2$ should be obtained [16]. In this case, analogous Argand plots of M'' vs. M' were made according to Eq. (8).

$$\left\{ M' - \frac{(M_U + M_R)}{2} \right\}^2 + (M'')^2 = \left(\frac{M_U - M_R}{2} \right)^2 \quad (8)$$

In M'' vs. M' plots the values proceed from lower to higher frequencies whereas in ϵ'' vs. ϵ' plots the values proceed from higher frequency to lower frequency. The Argand plots are shown in Figs. 7 and 8. Semicircular behavior is characteristic of the Debye model, in particular molecular liquids and small rigid molecules [16,31]. Polymers on the other hand deviate from semicircular behavior in which they exhibit a distribution of relaxation times and are often characterized by modified Cole–Cole expressions [16].

Fig. 7 shows the Argand plot in which data points were taken in the γ relaxation region. The plot does not follow

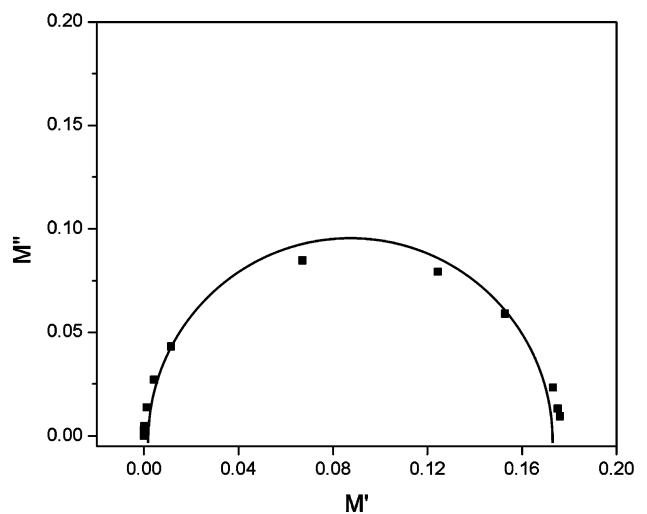


Fig. 8. Argand plot derived from the conductivity relaxation region (200°C).

semicircular behavior; this was expected, as this is a viscoelastic relaxation where entanglements due to chain interactions result in a distribution of relaxation times. Fig. 8 shows the Argand plot constructed with data taken at a temperature above T_g where the 2nd M'' peak is observed. This plot reveals a true semicircular arc, which can be interpreted to mean that it is indeed not a viscoelastic relaxation. Johari and Pathmanathan, together with others, have stated that conductivity relaxations in ionic conductors exhibit single relaxation times [19,20,22]. □

Proof 2. Ambrus et al. presented the electric modulus in terms of time, frequency and modulus [19]. Derivations have been shown in detail in various papers in which an expression for the electric modulus (M), Eq. (9), was determined under the assumption of conditions where ionic conduction is purely due to the diffusion of ions and independent of viscoelastic, dipolar relaxation [19,20,22,23, 29]. This assumption implies that under the stated conditions the electric modulus (M) will have a relaxation with a single relaxation time, τ_σ .

$$M = M_s \left(\frac{i\omega\tau_\sigma}{1 + i\omega\tau_\sigma} \right) = M_s \left[\frac{(\omega\tau_\sigma)^2}{1 + (\omega\tau_\sigma)^2} \right] + iM_s \left[\frac{\omega\tau_\sigma}{1 + (\omega\tau_\sigma)^2} \right] \quad (9)$$

In Eq. (9) $M_s = 1/\epsilon_s$ where ϵ_s occurs at a value of ϵ' that is independent of temperature. Starkweather Jr. et al. showed that plots of $\log M''$ and $\log M'$ vs. \log frequency will reveal slopes of 1 and 2, respectively [23]. In this study the dependence of M' , M'' on frequency in the conductivity relaxation region is shown in Figs. 9 and 10. As expected the plots reveal slopes of 1 and 2 at temperatures in the region of the conductivity relaxation. Similar plots were not obtained

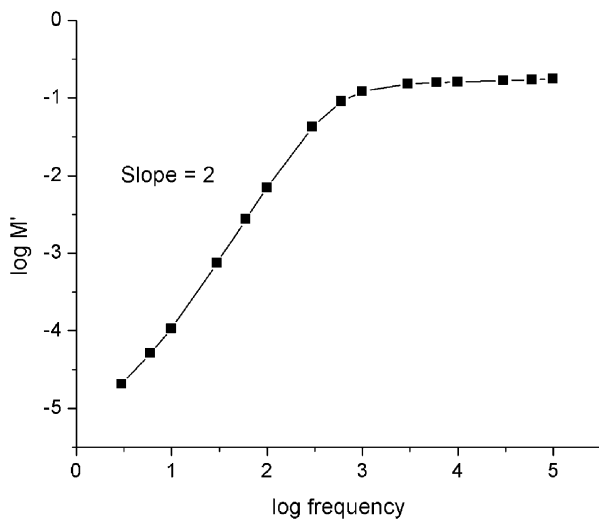


Fig. 9. Dependence of M' on frequency in the conductivity relaxation region (165 °C).

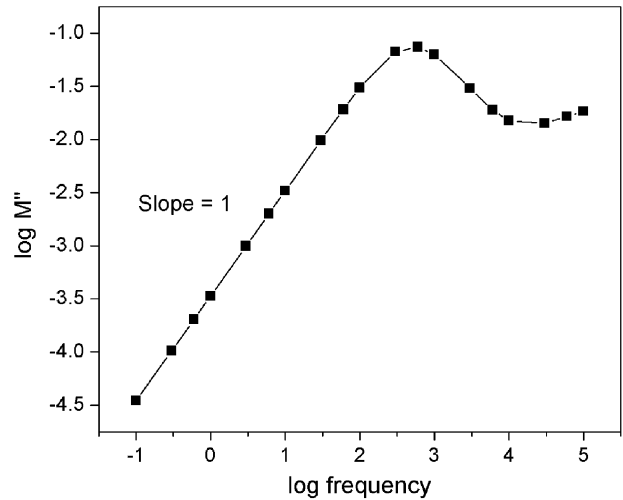


Fig. 10. Dependence of M'' on frequency in the conductivity relaxation region (165 °C).

for temperatures in the glass transition region and below. □

Proof 3. As mentioned earlier, two processes contribute to the loss factor. When viscoelastic effects are negligible, the loss factor is described by Eq. (2) [30,32,33]. Fig. 11 shows a plot of the frequency dependence of Ac conductivity (σ_{Ac}) for temperatures above T_g where conductivity is predominant. Dc conductivity (σ_{Dc}) was obtained by extrapolation to zero frequency. At low frequencies σ_{Ac} is independent of frequency from 110 to 200 °C. As temperature is increased, the frequency dependence of Ac conductivity plateaus and is independent of all frequencies measured. σ_{Dc} increased with increasing temperature and its Arrhenius relationship is expressed by Eq. (10), where E is the apparent activation energy, k is Boltzmann's constant and σ_o is the pre-exponential factor [34].

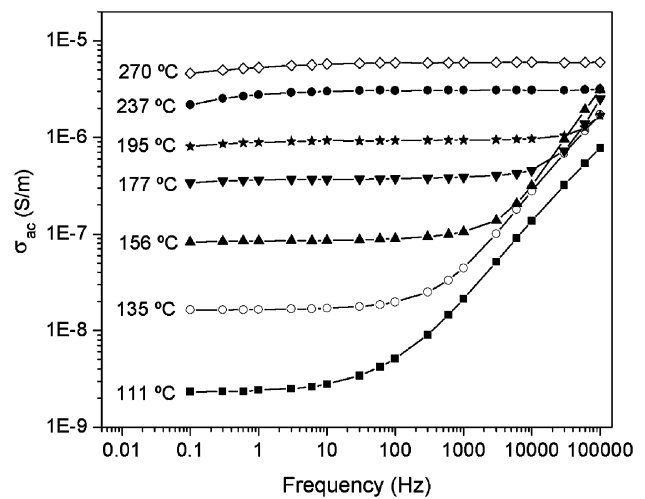


Fig. 11. Frequency dependence of Ac conductivity for PHEMA at temperatures above T_g .

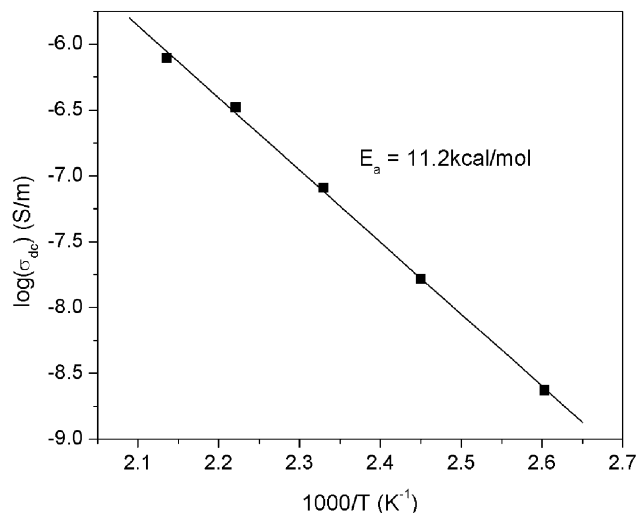


Fig. 12. Arrhenius plot of log Dc conductivity vs. the inverse of temperature.

$$\log \sigma_{\text{Dc}} = \log \sigma_0 \exp\left(\frac{-E}{kT}\right) \quad (10)$$

Pissis et al. reported that the ionic conductivity peak shows the same temperature dependence as Dc conductivity; Figs. 12 and 13 are used to compare the temperature dependence of the M'' peak and Dc conductivity [30,32]. The apparent activation energies determined from both plots are very close in value where the activation energy from the second M'' peak observed at high frequencies is 13.7 kcal/mol (57.4 kJ/mol) as compared to 11.2 kcal/mol (46.9 kJ/mol) obtained from the Dc conductivity plot. Only three frequencies (3000, 6000 and 10,000 Hz) were used to construct the Arrhenius plot for Fig. 13 since these are the only frequencies in which the two M'' peaks were clearly separated. Similar results have been reported in other systems [30,32]. □

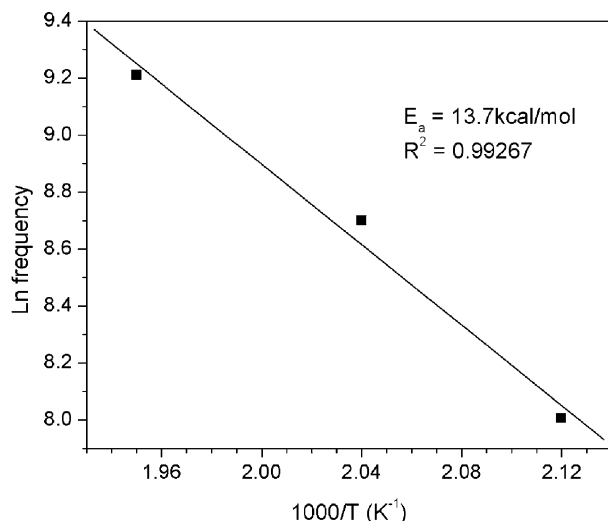


Fig. 13. Arrhenius plot of the conductivity M'' peak.

4. Conclusion

The dielectric spectrum of PHEMA has been examined in which the electric modulus formalism has been applied to the analysis of data. The γ relaxation region has been previously reported on by various authors. This study has presented analysis of the dielectric spectra in a temperature region up to and above the glass transition temperature to reveal the secondary β relaxation, the primary α relaxation and the conductivity relaxation. Several approaches were successfully applied to verify the presence of the conductivity relaxation. Further development and understanding of ionic conductivity in polymer composites is now underway.

Acknowledgements

This work was supported in part by the National Institute of Health (Grant # 5R01EB001640-02). The authors would like to thank J. Ors and P. Benz at Benz Research and Development (Sarasota, FL) for their generous supply of 2-HEMA monomer. We would also like to thank M. Zaworotko for the use of the TGA and B. Knudsen for DEA maintenance and repair.

References

- [1] Ratner BD, Hoffman AS. Hydrogels for biomedical applications. In: Andrade JD, editor. Hydrogels for medical and related applications. ACS symposium series, vol. 31. Washington: American Chemical Society; 1976. p. 1–36.
- [2] Meakin JR, Hukins DWL, Imrie CT, Aspden RM. *J Mater Sci-Mater M* 2003;14:9–15.
- [3] Gates G, Harmon JP, Ors J, Benz P. *Polymer* 2003;44(1):207–17.
- [4] Craig DQM, Tamburic S. *Eur J Pharm Biopharm* 1997;44:61–70.
- [5] LaPorte RJ. Hydrophilic polymer coatings for medical devices. Pennsylvania: Technomic; 1997.
- [6] Shtilman MI. Polymeric biomaterials: part1-polymer implants. New concept in polymer science series. Boston: VSP; 2003.
- [7] Diaz Calleja R. *J Polym Sci, Part B: Polym Phys* 1979;17:1395–401.
- [8] Gomez Ribelles JL, Diaz Calleja R. *J Polym Sci, Part B: Polym Phys* 1985;23:1297–307.
- [9] Russell GA, Hiltner PA, Gregonis DE, deVisser AC, Andrade JD. *J Polym Sci, Part B: Polym Phys* 1980;18:1271–83.
- [10] Pathmanathan K, Johari GP. *J Polym Sci, Part B: Polym Phys* 1990; 28:675–89.
- [11] Johari GP. *J Mol Struct* 1991;250:351–84.
- [12] Janacek J. *J Macromol Sci-Rev M* 1973;9(1):1–47.
- [13] Kolarik J. In: Cantow HJ, Dall'Asta G, Dusek K, Ferry JD, Fujita H, Gordon M, Kennedy JP, Keon W, Okamura S, Overberger CG, Saegwa T, Schulz GV, Slichter WP, Stille JK, editors. Secondary relaxations in glassy polymers. Advances in polymer science, vol. 46. New York: Springer; 1982. p. 119–61.
- [14] Kyritsis A, Pissis P, Gomez Ribelles JL, Monleon Pradas M. *J Non-Cryst Solids* 1994;172–174:1041–6.
- [15] Pathmanathan K, Johari JP. *J Chem Soc Faraday Trans* 1994;90(8): 1143–8.
- [16] McCrum NG, Read BE, Williams G. Anelastic and dielectric effects in polymeric solids. New York: Dover; 1967.

- [17] Avakian P, Starkweather Jr HW, Kampert WG. In: Cheng SZD, editor. Dielectric analysis of polymers. Handbook of thermal analysis and calorimetry, vol. 3. New York: Elsevier; 2002. p. 147–64.
- [18] TA Instruments, DEA 2970 Dielectric Analyzer, TA-057, TA instruments applications library: www.tainst.com.
- [19] Ambrus JH, Moynihan CT, Macedo PB. J Phys Chem 1972;76(22): 3287–95.
- [20] Johari GP, Pathmanathan K. Phys Chem Glasses 1988;29(6):219–24.
- [21] Bergman R, Alvarez F, Alegria A, Colmenero J. J Chem Phys 1998; 109(17):7546–55.
- [22] Macedo PB, Moynihan CT, Bose R. Phys Chem Glasses 1972;13(6): 171–9.
- [23] Starkweather Jr HW, Avakian P. J Polym Sci, Part B: Polym Phys 1992;30:637–41.
- [24] Nicolais L, Acierno D, Stol M, Janacek J. J Polym Sci, Part B: Polym Phys 1974;12:2579–81.
- [25] Gomez Ribelles JL, Diaz Calleja R. J Macromol Sci-Phys 1984; B23(2):255–69.
- [26] Gedde UW. Polymer physics. New York: Chapman&Hall; 1995.
- [27] Hartwig G. Polymer properties at room and cryogenic temperatures. New York: Plenum Press; 1994.
- [28] Mohsen NM, Craig RG, Filisko FE. J Oral Rehabil 2000;27:250–68.
- [29] Tsangaris GM, Psarras GC, Kouloumbi N. J Mater Sci 1998;33: 2027–37.
- [30] Pissis P, Kyritsis A. Solid State Ionics 1997;97:105–13.
- [31] Emran SK, Newkome GR, Weis CD, Harmon JP. J Polym Sci, Part B: Polym Phys 1999;37:2025–38.
- [32] Pissis P, Kyritsis A, Georgoussis G, Shilov VV, Shevchenko VV. Solid State Ionics 2000;136–137:255–60.
- [33] Henn F, Devautour S, Maati L, Giuntini JC, Schaefer H, Zanchetta JV, Vanderschueren J. Solid State Ionics 2000;136–137:1335–43.
- [34] Polizos G, Kyritsis A, Shilov VV, Shevchenko VV. Solid State Ionics 2000;136–137:1139–46.